The release of FB_1-induced heterophil extracellular traps in chicken is dependent on autophagy and glycolysis

Hanpeng Wu,[1] Xingyi Zhu,[1] Zhikai Wu, Peixuan Li, Yichun Chen, Yingrong Ye, Jingjing Wang, Ershun Zhou,[2] and Zhengtao Yang

College of Life Sciences and Engineering, Foshan University, Foshan 528225, Guangdong Province, PR China

ABSTRACT Fumonisin B_1 (**FB_1**), a worldwide contaminating mycotoxin produced by *Fusarium*, poses a great threat to the poultry industry. It was reported that extracellular traps could be induced by FB_1 efficiently in chickens. However, the relevance of autophagy and glycolysis in FB_1-triggered heterophil extracellular trap (**HET**) formation is unclear. In this study, immunostaining revealed that FB_1-induced HETs structures were composed of DNA coated with histones H3, and elastase, and that heterophils underwent LC3B-related autophagosome formation assembly driven by FB_1. Western blotting showed that FB_1 downregulated the phosphorylated phosphoinositide 3-kinase3-kinase (**PI3K**)/protein kinase B (**AKT**)/mechanistic target of rapamycin complex 1 (**mTORC1**) axis and raised the AMP-activated kinase α (**AMPKα**) activation protein. Furthermore, rapamycin- and 3-Methyladenine (**3-MA**)-treatments modulated FB_1-triggered HET formation according to the pharmacological analysis. Further studies on energy metabolism showed that glucose/lactate transport and glycolysis inhibitors abated FB_1-induced HETs. These results showed that FB_1-induced HET formation might interact with the autophagy process and relied on glucose/monocarboxylic acid transporter 1 (**MCT1**) and glycolysis, reflecting chicken's early innate immune responses against FB_1 intake.

Key words: fumonisin B_1, heterophil extracellular traps, chicken, autophagy, glycolysis

2023 Poultry Science 102:102511
https://doi.org/10.1016/j.psj.2023.102511

INTRODUCTION

Fumonisin B_1 (**FB_1**), the most common type of the 4 fumonisins, is mostly generated by the *Fusarium verticillioide,* which is often found in corn, wheat, and other cereals (Thiel et al., 1992). It is less prone to degrade during storage and manufacture due to its thermal stability and water solubility (Scott, 1993; Ponce-Garcia et al., 2018). Cereal is the major chicken feed, and the FB_1 toxicity to chicken immunity is often neglected. It is well known that substantial toxicity is caused by FB_1 suppression of ceramide synthase, which perturbs sphingolipid concentrations and might impact the inflammatory cell membrane (Arai et al., 1998). However, the role of FB_1 in innate immunity toxicity remains unknown.

Heterophils, like neutrophils, are the most abundant innate immune effector cells in the early, strong innate immune response of chicken. The heterophils manufacture the extracellular traps (**ETs**), namely heterophil extracellular traps (**HETs**), whose structures are well-demonstrated to date. A previous research has shown that FB_1 could increase the total ROS production in heterophils, including hydroxyl radicals (•OH) and nitrogen dioxide (•NO2), while extruding the HETs (Wu et al., 2022). Importantly, oxidative stress of FB_1 induces cellular autophagy (Chen et al., 2021). Autophagy is a degradation process that is responsible for the removal of damaged organelles or denatured proteins within cells, as well as protecting them from external stressors. That is why autophagy would maintain the homeostasis and survival of the heterophils to some extent (Filomeni et al., 2015). Thus, how autophagy primes heterophil to undergo HET formation against FB_1 fascinates us. Fortunately, the highly conserved autophagy program gives us a rare glimpse of its involvement at HET formation.

Despite the growing body of research on autophagy-related proteins such as mTOR, most studies of FB_1 administration are conducted without the immune cells. Autophagy was formerly considered to fuel the ETs formation. However, autophagy in bovine neutrophils and ATG5-knock out mice neutrophils parallels NETs

Received October 4, 2022.
Accepted January 13, 2023.

[1]These authors contributed to this work equally.

[2]Corresponding author: zhouershun@fosu.edu.cn

extrusion (Germic et al., 2017; Zhou et al., 2019). Autophagy in heterophils is poorly understood, let alone with FB_1 administration. Several studies pointed out that sphingolipid accumulation, one of the FB_1 targets, impacts the AMPK-mTOR signaling pathway (Knupp et al., 2017). Also, AMPK and mTOR regulate autophagy by monitoring the need for glucose, amino acids, and ATP. These characteristics lead us to investigate the integrated signaling network.

Autophagy is characterized as mTOR dependent/independent pathways depending on the function of the initiators: the former, PI3K/Akt/mTORC1 axis, focuses on amino acid concentration (Jewell et al., 2013); the latter, ULK1/AMPKα axis, which is a direct signal to sense the ATP demand (Li and Chen, 2019). The purpose of this section was to see if Class I PI3K/Akt/mTORC1 and AMPKα/ULK1 are engaged in FB_1 stimulation. Because LC3-I is transformed to LC3-II by lipidation, allowing LC3 to link with autophagic vesicles during autophagy, the detectable fluorescence signal of LC3-II is utilized as an indication of autophagosomes (Tanida et al., 2008). Early in autophagy, in addition to the conjugation of the protein Atg8/LC3 to phosphatidylethanolamine as the key in defining an autophagosome as a distinct organelle, the autophagy-specific class III PI3K produces phosphatidylinositol-3-phosphate (**PI3P**). Until the discovery of double FYVE−containing protein 1, which mediates PI3P binding capacity, pre-autophagosomal structure membrane came from different organelle mechanisms that gradually gained acceptance (Axe et al., 2008); the recruited Class III PI3K to facilitate pre-autophagosomal structure elongation through PI3P synthesis, which is the key event of the autophagosome formation. Thus, the role of class III PI3K and LC3B expression in FB_1-induced autophagosome formation is critical in our study.

Autophagy and neutrophil metabolism seem to interact, according to growing data. Fructose-2,6-biphosphatase 3 (**PFKFB3**) promoted autophagy through the AMPK signaling pathway (Yan et al., 2017). AMPK pathways are also implicated in stress-induced glucose transporter 4 (**GLUT4**) and GLUT1-mediated glucose uptake (Barnes et al., 2002; Frøsig et al., 2010), implying that autophagy is linked to glucose transport and glycolysis. On the other hand, there are 2 metabolic phases of NETosis. The first is independent of exogenous glucose, followed by glycolysis and exogenous glucose (Rodríguez-Espinosa et al., 2015). That being said, glycolysis and exogenous glucose uptake are likely involved in the NET formation. Because of the unique metabolism of heterophil, NETosis is tightly connected to glycolysis. Although autophagy and FB_1-induced HET formation relationship are unclear, some studies indicated that hexokinase II (**HK2**) is an example that facilitates autophagy in response to glucose deprivation by mTORC1 (Tan and Miyamoto, 2015). Moreover, inhibiting HK2 would keep the HET formation at bay (Jiang et al., 2021). Nevertheless, NETosis metabolism is currently poorly understood. We used the 2 types of inhibitors, one concentrating on energy substances transport on the heterophil membrane and the other on the nodal sites of the glycolysis in heterophil, to investigate the energy needs for FB_1-induced HETs release. We wonder the role of critical metabolic pathways in FB_1-induced chicken HET release.

MATERIALS AND METHODS

Isolation of Chicken Heterophils

Healthy adult welsummer roosters (n = 5, 14−18 wk old, 1−1.5 kg) served as blood donors. The peripheral blood was collected from the large vein under the wing (brachial vein) with sterile glass tubes containing $EDTAK_2$. Then chicken heterophils were isolated by the commercially available Chicken Heterophils Isolation Kit (Cat. #LZS1098C, TianJin HaoYang Biological Manufacture Co., Ltd, China). Briefly, blood was diluted 1:1 phenol red-free medium containing 5.56 mM glucose without glutamine (RPMI Medium 1640, Cat. #90022, Solarbio, Beijing, China), layered on a separating solution in centrifugal tubes, and then centrifuged at 900 *g* for 50 min. The lower cellular layer, consisting mainly of heterophils and erythrocytes, was collected and then washed with erythrocyte lysis solution until the cell mass turned white. After centrifugation at 650 *g* for 15 min, supernatant was discarded. Finally, freshly purified heterophils (≥ 90% of the cell) from the bottom of the centrifugal tubes were resuspended in 1,640 medium for subsequent experiments. They rested at 5% CO_2 and 37°C atmospheres until further use. For heterophils counting, we took trypan blue-treated cell suspension using a pipette and applied it to the glass hemocytometer, the percentage of living cells was over 95%.

We set up 5 biological replicates and 2 technical replicates for each experiment. Notably, each rooster was collected approximately 7 mL of peripheral blood each time, according to body weight and circulating blood volume. Analysis of cell samples from multiple chickens was treated independently. Techniques of operations require gentle handling in the whole process.

All procedures complied with the Guide for the Care and Use of Laboratory Animals published by the National Institutes of Health and approved by the Institutional Animal Care and Use Ethics Committee of Foshan University (Permit NO. SCXX (yue) 2022-0061).

Heterophil Viability Assays

Heterophils suspension were inoculated (2×10^5/mL) in a 96-well plate and stimulated with 40 μM FB_1 (Cat. #Z2125, Sigma-Aldrich, Germany) for 1.5 h. Then 10 μL Cell Counting Kit reagent containing WST-8 (water-soluble tetrazolium, monosodium salt) was added into each well according to manufacturer's instructions (Cat. #GK10001, GLPBIO) and the plate was incubated at 37°C. Lastly, the absorbance was measured at 450 nm by the iMark microplate absorbance

reader (Bio-Rad, Serial No. 18855, Japan). The absorbance of the experimental well (absorbance of cells, medium, CCK8, and wells of the test compound) is denoted as As. The blank well absorbance (absorbance of wells containing medium and CCK8) is represented as Ab. The control well absorbance (absorbance of wells containing cells, medium, and CCK8) is denoted as Ac. Thus, the viability of the heterophil is

$$\text{Cell viability}\,(\%) = [(\text{As} - \text{Ab})/(\text{Ac} - \text{Ab})] \times 100 \quad (1)$$

Microscopic Examination of HET Formation Via Immunostaining

The heterophils (2×10^5/well) were stimulated with FB_1 (40 μM) for 1.5 h at 37°C on coverslips (14 mm diameter, Biosharp, China) pretreated with poly-$_L$-Lysine (0.1 mg/mL, Sigma-Aldrich, Germany). Then, the samples were fixed with 4% (w/v) paraformaldehyde (Beijing Labgic Technology Co., Ltd, China) and stored at 4°C until further experiments. For HET visualization, the fixed samples were washed in PBS thrice, permeabilized with 0.2% Triton X-100 for 20 min, blocked in 3% goat serum, and soaked in primary antibody solution (H3 and NE, 1:200, 4°C) overnight. The antibodies were diluted to 1:200 with 3% goat serum, respectively. After thrice washing with PBS, the samples were incubated with the second conjugated antibody (goat anti-rabbit IgG, FITC, Absin Bioscience Inc., China) for 1.5 h, then incubated with 5 mM Sytox Orange (Invitrogen) for 20 min. (Citrulline R2 + R8 + R17) Anti-Histone H3 antibody (ab5103; Abcam, UK) and Anti-Neutrophil Elastase (NE) antibody (ab68672; Abcam, UK) were used in the experiments. The visualization was achieved using an inverted fluorescence microscope (DISCOVER ECHO Inc.) equipped with Flat Field Semi-Complex Achromatic objective. Image processing was carried out with Fiji ImageJ using merged channel plugins and restricted to overall adjustment of brightness and contrast.

Autophagosome Detection by Immunofluorescence Analysis

Analysis of autophagosome formation in heterophils was performed according to Itakura and McCarty (Itakura and McCarty, 2013). For autophagosome detection, fixed cells were washed in PBS 3 times, permeabilized ice-cold methanol treatment (3 min at 4°C), and blocked with blocking buffer (5% BSA, 0.1% Triton X-100 in sterile PBS) for 60 min at RT. After that, cells were soaked overnight at 4°C in an anti-LC3B antibody solution (Cat. #2775 Cell Signaling Technology) diluted 1:200 in a blocking buffer. After incubation, samples were washed 3 times with PBS and incubated for 30 min in the dark and RT in the secondary antibody (goat anti-rabbit IgG, FITC, 1:200, diluted with blocking solution; Cat. #SA00003-2, Proteintech Group, Inc.). After 3 washes in PBS, samples were mounted and incubated with 5 mM Sytox Orange (Invitrogen) for 20 min. Images were taken applying the fluorescent microscope (Model: RVL-100-G, DISCOVER ECHO Inc.) equipped with Flat Field Semi-Complex Achromatic objective. Image processing was carried out with Fiji ImageJ using merged channel plugins and restricted to overall adjustment of brightness and contrast.

Western Blot Analysis

Heterophils (2×10^5/well) were stimulated with FB_1 (40 μM) for 1.5 h in 5% CO_2 at 37°C atmospheres and then lysed with mammalian protein extraction reagent (Thermo Fisher Scientific) at 4°C. After centrifugation at 12,000 g at 4°C by a High-speed refrigerated centrifuge (Model: 5424R, Eppendorf, Germany), the supernatant was collected. The total protein concentration was assayed with the bicinchoninic acid (**BCA**) protein assay kit (Cat. #23225, Thermo Fisher Scientific). Samples with equal amounts of protein were separated by sodium dodecyl sulfate-polyacrylamide gel electrophoresis (Model: PowerPac HC, Bio-Rad, Singapore) and transferred to a polyvinylidene difluoride membrane (0.45 μm Cat. #IPVH00010, MerckMillipore, Burlington, MA). The membranes were blocked in 3% bovine serum albumin (**BSA**) for 1 h at room temperature and probed with primary antibodies 1:2,000 diluted in blocking solution at 4°C overnight. The next day, membranes were washed 3 times with TBST for 10 min and then incubated with HRP-conjugated secondary antibody (1:20,000 dilution in TBST) for 1 h at room temperature. Finally, membranes were washed 3 times for 10 min and visualized with Bioanalytical Imaging System (Azure Biosystems, Inc., CA). Immobilon Western chemiluminescent HRP Substrate (Merck Millipore) was used for chemiluminescence detection.

The following primary antibodies, anti-phospho-Akt mAb (Cat. #4060), anti-Akt mAb (Cat. #4691), anti-p-mTOR mAb (Cat. #5536), anti-mTOR mAb (Cat. #2983), anti-PI3K class III mAb (Cat. #3358), anti-p-AMPK mAb (Cat. #2535), anti-AMPK mAb (Cat. #5832), anti-ULK1 mAb (Cat. #8054), anti-p-ULK1 pAb (Cat. #6888), and anti-LC3B mAb (Cat. #3868) were purchased from Cell Signaling Technology, anti-phospho-PI3K p85 alpha (Cat. #bs-3332R), anti-PI3K p85 alpha antibody (Cat. #bsm-52219M) were purchased from Bioss. The protein level was normalized with β-actin expression with a β-actin polyclonal antibody (1:1,000, Cat. #132001, Absin Bioscience Co Ltd., Shanghai, China). Quantification of protein band intensities was performed using Image J software 1.48 version.

Quantitation of HETs

Heterophils were pretreated with inhibitors for 30 min in a 96-well microplate and then challenged by RPMI 1640 medium (as control), FB_1 (40 μM), or zymosan (1 mg/mL, as positive control) for 1.5 h at 37°C and 5% CO_2 atmosphere. For sampling methods, a 1:200

dilution of Picogreen (Invitrogen) in 10 mM Tris-HCl buffered with 1 mM EDTA (Life Technologies Corporation) was added to each well (50 μL), 15 min after adding Picogreen solution. The plate was read by the Infiniti M200 fluorescence plate reader (Tecan, Austria) with 484 nm excitation/525 nm emission.

The inhibitor of mTOR (Rapamycin, 50 μM) was purchased from MedChemExpress. The following inhibitors of PI3K class III (3-MA, 10 μM), GLUT1 (STF-31, 1 μM), PFKFB3 enzyme (3PO, 24 mM), MCT1 (AZD3965, 1.6 μM), GLUT4 (Ritonavir, 4.2 μM), HK2 (Bromopyruvic acid, 3 mM), RAC-GTPase (NSC23766, 1.6 μM) were purchased from Sigma-Aldrich. The concentrations of used inhibitors were based on our previous studies (Jiang et al., 2021).

Apoptosis Assay

The cells at the density of 2×10^6 cells/mL were seeded into 6-well plates and incubated with 40 μM FB_1 for 1.5 h. The apoptosis of heterophils was detected by the commercially available Apoptosis Kit (Cat. #BL100A, Beijing Labgic Technology Co., Ltd). The practical steps followed the manufacturer's instructions. Briefly, we prepared 1 × binding buffer by mixing 1 part of 4 × binding buffer with 4 parts of distilled water. The heterophils were harvested at centrifuge tubes and washed with cold PBS, followed by being centrifuged at 1,500 rpm for 5 min. Subsequently, the cells were resuspended with 100 μL 1 × binding buffer and incubated with 5 μL of annexin-V labeling solution for 10 min at room temperature in the dark. Five minutes before being placed on the flow cytometer, 10 μL of Propidium Iodide (**PI**) Staining Solution and 400 μL PBS was added, and the results were analyzed on a flow cytometer (Model: A00-1-1102; Beckman Coulter Biotechnology Co., Ltd).

Statistical Analysis

All Data were expressed as mean ± SEM. Graphs and statistical analyses were performed by Graphpad Prism 9. This paper used the one-way analysis of variance (**ANOVA**) or student *t* test. Statistical significance was defined by a P-value < 0.05.

RESULTS

FB_1 Had No Effect on the Viability of Chicken Heterophils

Due to the toxicity of trypan blue, the findings of heterophils stained with it cannot identify whether heterophil viability changes. The WST-8 test, which generates matching formazan orange dye, is used to measure neutrophil activity and offer more quantitative data. After 1.5 h of treatment with 40 μM FB_1, cell viability did not change substantially ($P > 0.05$), showing that FB_1 did not affect chicken heterophil viability (Figure 1).

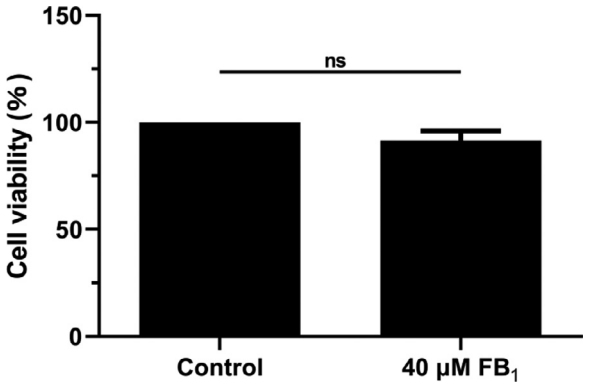

Figure 1. FB_1 did not affect the viability of the heterophils. Heterophils were incubated with 40 μM FB_1 for 1.5 h. Then cell counting reagent was added and incubated for 1 h. Finally, its absorbance was detected at the wavelength of 450 nm. Each value was represented as mean ± SEM (n = 5). The student's *t* test was used to determine the significance ("ns" means no significant differences).

FB_1 Exposure Triggered HET Formation in Chicken

Indirect immunofluorescence staining is a straightforward method for studying HET structure. To verify that chicken heterophils were indeed undergoing HET formation, the main components of HETs (i.e., citrullinated histone H3 or Elastase) were immunolabeled. Co-localization analyses of extracellular DNA decorated with citrullinated histone H3 or elastase in FB_1-induced structures. As shown in Figure 2, we also observed HET formation driven by zymosan. HET structures (indicated by white arrows) were co-localized by DNA, citrullinated histone H3 or elastase staining in the merged images.

FB_1 Exposure Triggered Autophagosomes Formation in Chicken Heterophils

We also looked at how FB_1 exposure affected the heterophil-derived autophagosome formation. We, therefore, used an antibody directed against the splice variant LC3B as a marker to study the impact of FB_1 exposure to heterophil-derived autophagy and of autophagy on FB_1-induced HET formation. Figure 3 showed that FB_1 exposure resulted in significant autophagosome formation in subjected chicken heterophils compared to that of control group. Notably, LC3B-positive and NETotic heterophil against FB_1 were captured at the same location in the merged picture, demonstrating a positive association between HET formation and autophagy in FB_1-exposed chicken heterophil.

FB_1 Downregulated the Phosphorylation of PI3K/Akt/mTOR Proteins in Chicken Heterophils

Activation of the mTOR signaling pathway is useful for understanding/evaluating the link between NETosis

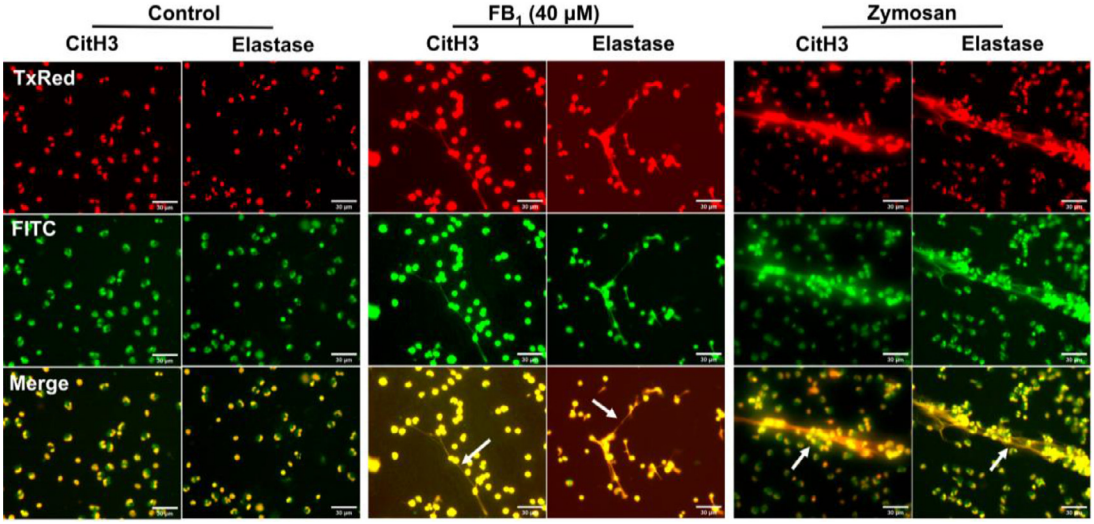

Figure 2. HETs visualization. We seeded primary chicken heterophils (2×10^5/well) on glass coverslips pretreated with poly-$_L$-lysine (0.1 mg/mL) and incubated with FB_1 (40 μM) for 1.5 h in an incubator. Samples were fixed with 4% paraformaldehyde for 20 min, immunolabeled with antibodies directed against citH3 (FITC channel) or NE (FITC channel) for HETs, then incubated with Nucleic Acid Stain (TxRed channel). We observed and took images (200 ×) of the examples under the fluorescent microscope. White arrows indicated HETs structures in merged photos. Bars, 30 μm.

and autophagy, since mTOR-dependent autophagy and NETosis would occur independently (Zhou et al., 2019). In the upstream of the axis, PI3K is a heterodimer consisting of a regulatory subunit and a catalytic subunit. However, p85α, as the most abundant regulatory subunit of Class IA PI3K, remains elusive (Li et al., 2016). As shown in Figure 4, the phosphorylated p85 regulatory subunit of PI3K, Akt, and mTORC1 proteins were decreased significantly in mTOR-dependent pathways ($P < 0.01$), suggesting FB_1 influenced the PI3K/Akt/mTOR axis in FB_1-exposed chicken heterophil.

FB_1 Enhanced the Phosphorylation of AMPK α1/ULK1/PI3K Class III Proteins and LC3B Expression in Chicken Heterophils

AMPK, an autophagy activator, phosphorylates ULK1 at several sites. It seems that ULK1 may act as a point of convergence for several autophagy-controlling signals such as AMPK and mTOR. Endogenous levels of total AMPK α1/ULK1/Class III PI3K protein were detected in this section. We quantified endogenous levels of total LC3B protein after observing the LC3B-coated

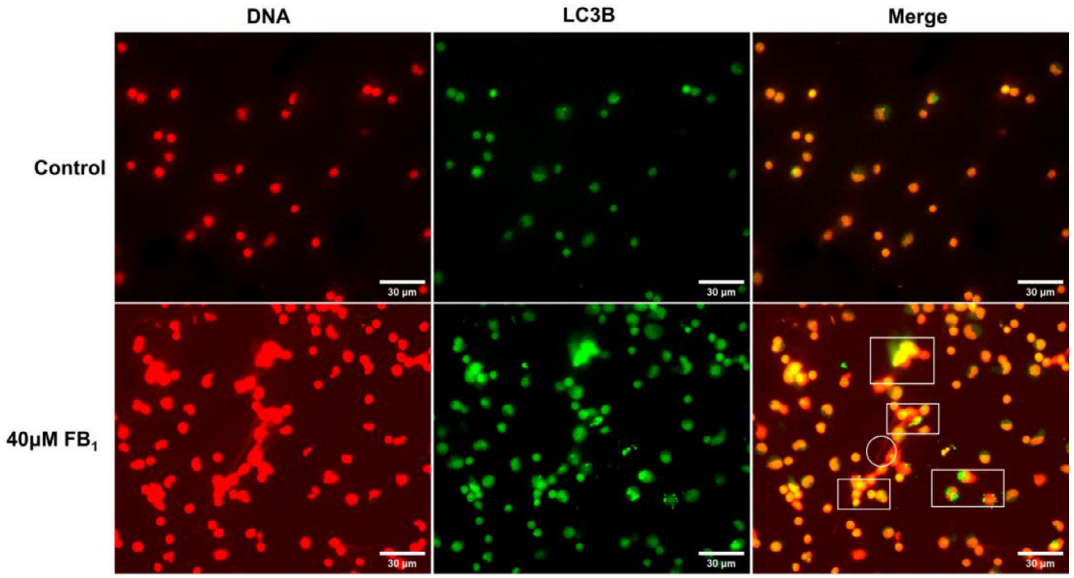

Figure 3. Autophagosomes visualization. We seeded primary chicken heterophils (2×10^5/well) on glass coverslips pretreated with poly-$_L$-lysine (0.1 mg/mL) and incubated with RPMI 1640 and FB_1 (40 μM) for 1.5 h in an incubator. Samples were fixed with 4% paraformaldehyde for 20 min, immunolabeled with antibodies directed against LC3B (FITC channel), and incubated with Nucleic Acid Stain (TxRed channel). Finally, mounted in the mounting medium. Samples were observed, and images (200 ×) were taken under the fluorescent microscope. The distribution of green fluorescence indicated autophagosome formation. In merged photos, white circles and rectangles suggested the shape of the autophagosome and extracellular traps in the meantime. Bars, 30 μm.

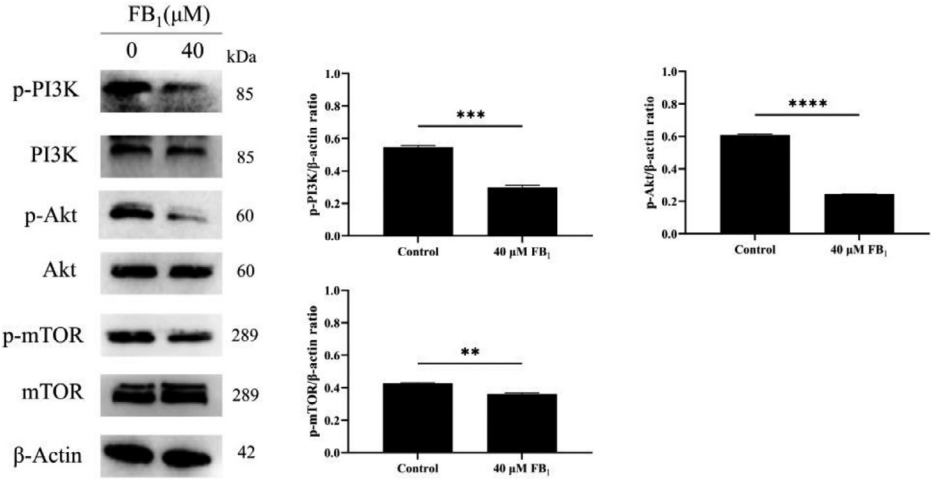

Figure 4. PI3K-Akt-mTOR phosphorylation. Heterophils (2×10^5/well) were administered after 40 μM FB_1 treatment for 1.5 h, total proteins were isolated, and the expression of p-PI3K, p-Akt, and p-mTOR in heterophil was analyzed by western blot by using the indicated antibodies. Data represent mean ± SEM (n = 5). Statistical analysis by student's t test (**$P < 0.01$, ***$P < 0.001$, ****$P < 0.0001$).

autophagosome. For illustration, stronger reactivity was observed with the type II form of LC3B ($P < 0.01$), albeit cross-reactivity with other LC3 isoforms may exist. Conclusively, phosphorylated AMPKα/ULK1/PI3K class III proteins and LC3B expression (Figure 5) were considerably elevated ($P < 0.01$), suggesting that FB_1 regulated AMPKα/ULK1-related protein in FB_1-exposed chicken heterophil.

The Formation of FB_1-Triggered HET Was Dependent on Autophagy in Chicken

The pharmacological experiment was performed to prove the relationship between autophagy and the HET formation from different angles under the FB_1 stimulation. As shown in Figure 6, we obtained increased HET formation after rapamycin exposure and decreased HET formation after 3-MA treatment ($P < 0.001$), indicating that autophagy played an important role in FB_1-triggered HET formation in chicken.

FB_1-Triggered HET Extrusion Was Dependent on Glucose Uptake and Glycolysis in Chicken Heterophils

Autophagy-related protein regulates heterophil metabolism in some ways. Here, compared with the control group, our present data (Figure 7) shows that HET extrusion triggered by FB_1 declined precipitously with the inhibitor of glucose transport of GLUT1 (STF-31, $P < 0.01$). Moreover, the glycolysis inhibitors of PFKFB3 (3PO, $P < 0.05$), MCT1 (AZD3965, $P < 0.01$) also reduced extracellular DNA release, implying that inhibition of the glucose uptake, and glycolysis may be the potential causes of the observed FB_1-triggered HET suppression.

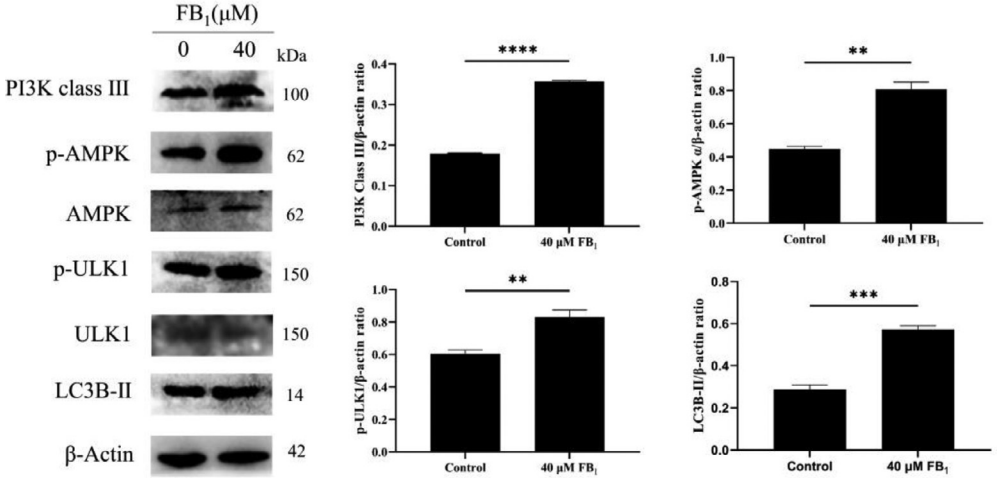

Figure 5. AMPK-ULK1 phosphorylation, PI3K class III, and LC3B protein expression. Heterophils (2×10^5/well) were administered after 40 μM FB_1 treatment for 1.5 h, total proteins were isolated, and the expression of p-AMPK and p-ULK1 in heterophil were analyzed by western blot by using the indicated antibodies. Data represent mean ± SEM (n = 5). Statistical analysis by student's t test (**$P < 0.01$, ***$P < 0.001$).

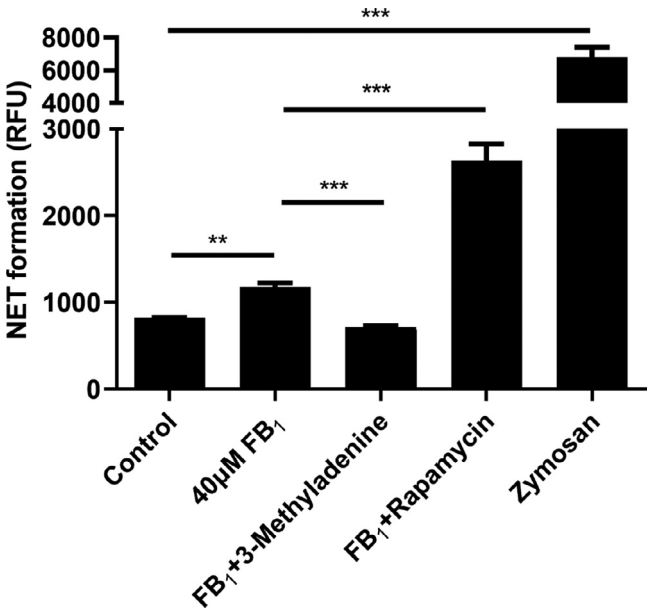

Figure 6. Autophagy mediated FB_1-triggered HET extrusion. We pretreated primary heterophils (2×10^5/well) for 30 min with the inhibitor of 3-MA and rapamycin in a 96-well microplate, followed by exposure to 40 μM FB_1 for 1.5 h. Each value was represented as mean ± SEM (n = 5). Statistical analysis by one-way ANOVA (**$P < 0.01$, ***$P < 0.001$).

Besides, we found that HET extrusion triggered by FB_1 declined sharply (Figure 8) with the inhibitor of glucose transport of GLUT4 (Ritonavir, $P < 0.01$), Rac GTPase (NSC23766, $P < 0.001$). The glycolysis inhibitors of hexokinase II (Bromopyruvic acid, $P < 0.01$) reduced extracellular DNA release compared to that of the control group, suggesting that the glucose uptake and glycolysis were crucial in FB_1-triggered HET formation in chicken.

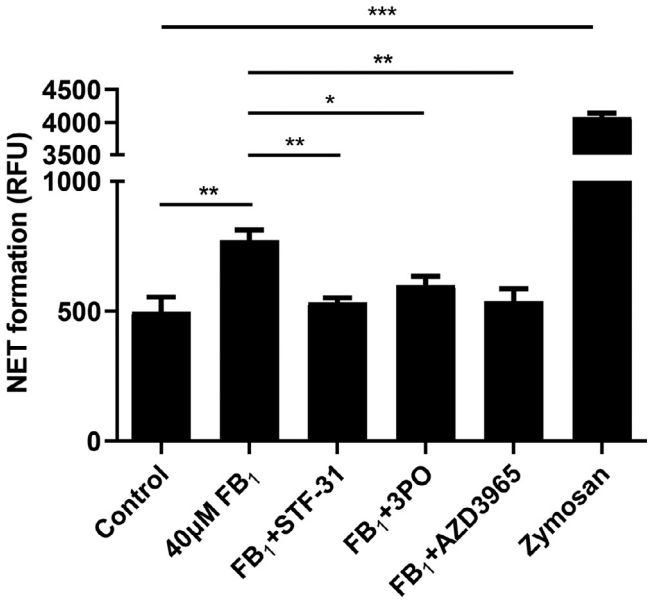

Figure 7. FB_1-induced HETs formation was dependent on GLUT1, PFKFB3, and MCT1. We pretreated primary heterophils (2×10^5/well) for 30 min with STF-31, 3PO, AZD3965 in a 96-well microplate, followed by the exposure to 40 μM FB_1 for 1.5 h. The positive control group was incubated with zymosan (1 mg/mL). Each value was represented as mean ± SEM (n = 5). Statistical analysis by one-way ANOVA (*$P < 0.05$, **$P < 0.01$, ***$P < 0.001$).

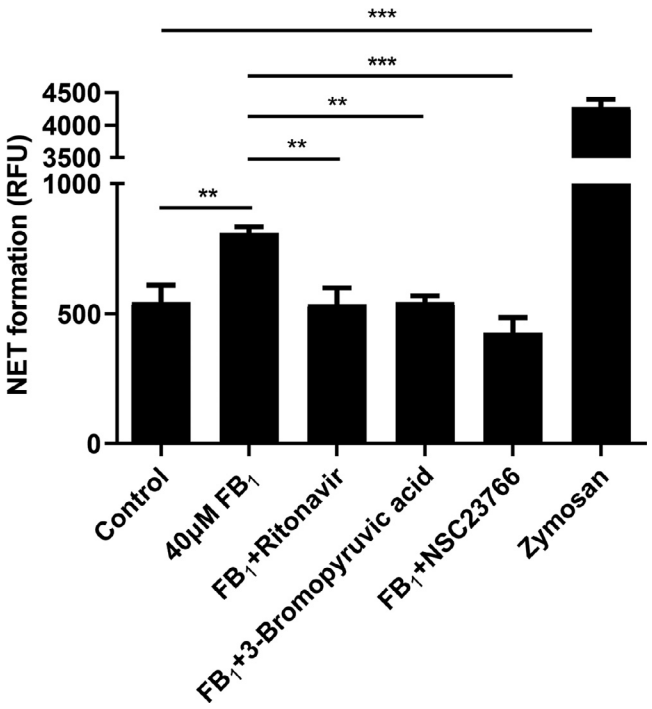

Figure 8. FB_1-induced HETs formation was dependent on GLUT4, HK2, and RAC-GTPase. We pretreated primary heterophils (2×10^5/well) for 30 min with Ritonavir, Bromopyruvic acid, and NSC23766 in a 96-well microplate, followed by the exposure to 40 μM FB_1 for 1.5 h. The positive control group was incubated with zymosan (1 mg/mL). Each value was represented as mean ± SEM (n = 5). Statistical analysis by one-way ANOVA (**$P < 0.01$, ***$P < 0.001$).

FB_1-Induced HET Formation Was Accompanied by No Apoptosis in Chicken

Aside from HETs, heterophils undergo cell apoptosis and necrosis. Using flow cytometry and annexin V/PI labeling, we investigated the effects of FB_1. Phosphatidylserine exposure on the cell membrane's external surface has been reported in the early stages of apoptotic cell death while the cell membrane is still intact. The alterations in phosphatidylserine asymmetry to the cell membrane cause the attachment of annexin V, which is related to apoptosis. PI colors dead cells red, binding tightly to the nucleic acids through the late apoptosis and necrosis cell membrane but is impermeant to live cells and the early apoptotic cells. After staining a cell population with FITC Annexin V and PI in the provided binding buffer, apoptotic cells show green fluorescence, and dead cells show red and green fluorescence. The flow cytometer can readily differentiate these groups. Figure 9 indicates that chicken heterophils show less apoptosis and necrosis compared to that in the control group ($P > 0.5$). The number of viable heterophils was unaffected ($P > 0.5$).

DISCUSSION

Takei et al. (1996) discovered a new kind of neutrophil death that was neither apoptosis nor necrosis in 1996. Until 2004, the first description of NET formation was published and known as ETosis nowadays

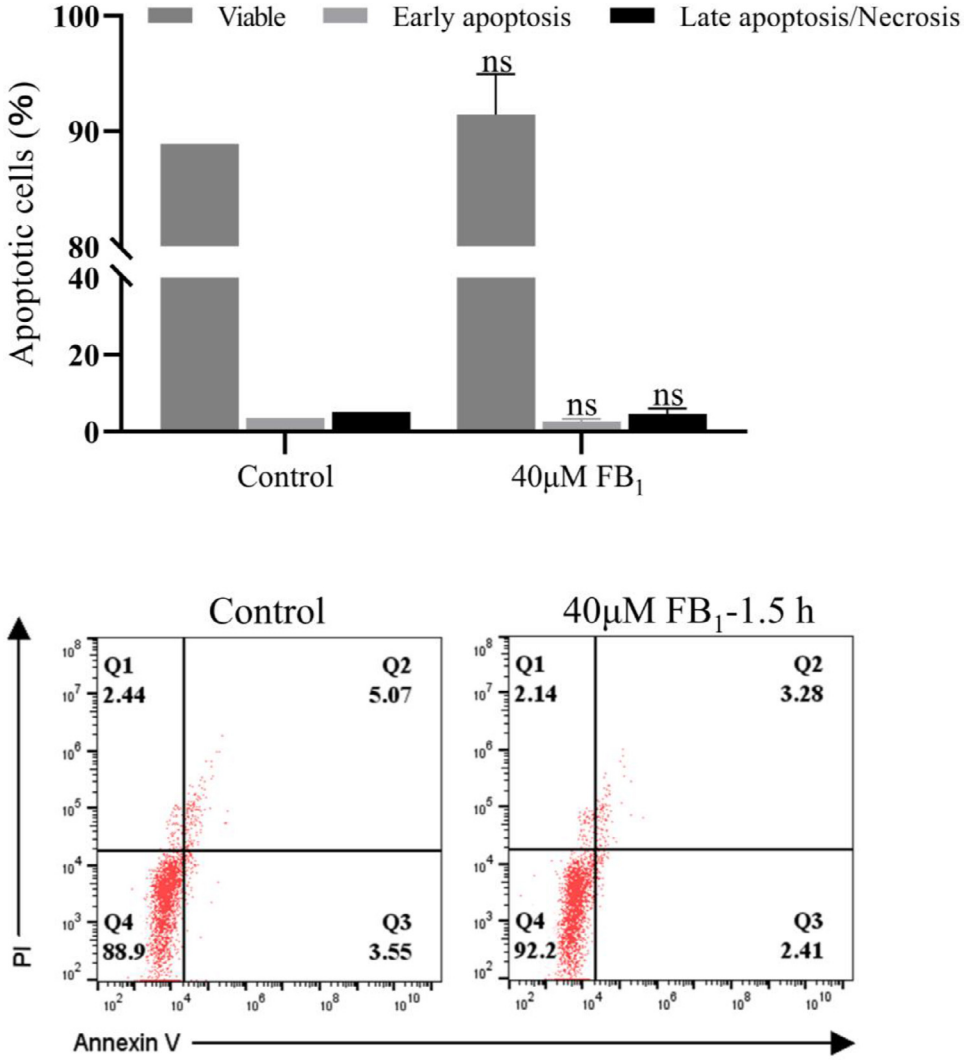

Figure 9. FB_1-induced HET formation is accompanied by no apoptosis. The cells were seeded into 6-well plates (2×10^6/well) and incubated with 40 μM FB_1 for 1.5 h, and apoptosis was assessed using annexin V/PI staining. The sample dot plots demonstrate varying ratios of apoptotic and necrotic cells. Q4 = viable cells; Q3 = early apoptotic cells; Q2 = late apoptotic cell/necrotic cells. Each value was represented as mean ± SEM (n = 5). The student's *t* test was used to determine the significance ("ns" means no significant differences).

(Brinkmann et al., 2004). Meanwhile, ETosis has been linked to a variety of diseases, including sterile inflammation, that is, human gout and bovine synovitis. So far, we knew very little about HETs in chicken.

In terms of stimulation, both chemicals and pathogens can cause ETosis. Several studies have demonstrated that mycotoxin, such as zearalenone, could efficiently induce ETosis. As the general inhibitor of ceramide synthases, FB_1 indirectly regulates the lactosylceramide, which accounts for nearly two-thirds of the glycolipid molecules in the neutrophil plasma membrane, hence weakening innate immunity (Arai et al., 1998). Recently, Wu et al. (2022) confirmed FB_1 as potent HET inducers by quantifying extracellular DNA with Picogreen. The current study aimed to investigate more closely at FB_1-triggered HET formation and analyze the intersections with autophagy/glycolysis in vitro. In the confrontation of FB_1, it is unclear how these 2 potential processes will occur during the HET formation. Given that 40 μM FB_1 stimuli for 1.5 h, as the trigger condition, will culminate with HET releasing, this might be the optimal condition for extended research based on previous studies (Wu et al., 2022). Overall, this study discussed the growing significance of autophagy in forming HETs both at the molecular level and within glycolysis.

Nevertheless, immunostaining analyses revealed that these extracellular structures were mainly composed of DNA being decorated with histones H3 and elastase, thereby confirming classical components of ETs, which is in line with our previous research (Wu et al., 2022). Additionally, autophagosomes were visualized. When the cell catabolizes intracellular proteins to acquire energy, autophagy occurs, although cellular stressors such as hunger would enhance autophagy. As a result, a little autophagosome may still be detected in the control group. Autophagosome formation was enhanced in the FB_1-treated group compared to that of control group. More importantly, autophagosomes and DNA, the skeleton of ETs, were caught at the same location, indicating that autophagy correlated with HET extrusion to some degree. Casting HETs is an ATP-driving process, which suggests that autophagy is at work behind the scenes.

Previous research indicated that FB_1 might cause apoptosis in a variety of cells. Our findings suggested that the process of FB_1-induced HET formation could also be accompanied by no apoptosis. Following that, we concentrated on determining the mechanism behind FB_1-induced heterophil autophagy. Though several studies in vitro have indicated macroautophagy (therefore autophagy) sequence-protein activation, the immune cell still needs experimental data. The mTOR-dependent and -independent pathways are primarily involved in the autophagy upstream signaling. mTOR is thought to be downstream of the PI3K/AKT signaling, detecting the requirement for nitrogen in the cell. The phosphorylation of PI3K p85α/Akt/mTOR axis increased considerably in this research. Based on previous studies, this signaling may begin with inhibiting PI3K class I, specifically, a catalytic subunit α that binds the p85 regulatory subunit and recruits AKT activation, then suppresses mTOR. One of the mTOR-independent pathways, AMPK is the sensor of cell's energy condition; instability causes like oxidative stress will activate AMPKα1, triggering cellular autophagy by activating ULK1 and maintaining homeostasis. ULK1 phosphorylation was enhanced as predicted. ULK1 also serves as an mTOR downstream enzyme during autophagosome formation (Kim et al., 2011). Finally, 2 types of pathways converge on the ULK1 complex, completing the initiation step (Figure 10).

Notably, immune cells express 3 classes of PI3K (Okkenhaug, 2013). This study focused on the stress sensor, class I PI3K, and the class III PI3K function in autophagy autophagosome. The PI3K class I signaling pathway inhibits autophagy, while the class III PI3K does the reverse. Our study implied that FB_1 could promote autophagosome elongation by upregulating class III PI3K. Meanwhile, the autophagosome is intermediate to the autolysosome; examining LC3B protein production in fluorescence microscopy is significant because the change of LC3 I to LC3 II-B reflects the autophagosome maturation (Tanida et al., 2008). In general, the result of Class III PI3K phosphorylation and LC3 II-B expression in western blot indicated that most phagophores had become mature organelle (Figure 10).

FB_1 triggered heterophil autophagy through mTOR dependent/independent pathway. We then used a pharmacological inhibitor/activator to see whether the HET formation relies on autophagy. This study found that 3-MA dramatically reduced HET formation, proving that autophagy is associated with HET formation. Some studies argued that NETosis was dependent on the NADPH oxidase activation (Yousefi et al., 2009), which needs PI3K class I activity (Geering et al., 2011), and 3-MA does not discriminate between different PI3K isoforms, for instance, blocking both class III and I PI3K activity (Germic et al., 2017). In other words, it is hard to define if NETosis is disrupted by the autophagosome inhibitor or NAPDH oxidase activity was suspended, resulting in an unwarranted conclusion. It should be mentioned that oxidative stress is an inevitable part of NETosis, and its resources are varied. Confrontation of bovine neutrophils and chicken heterophils with FB_1 resulted in a significant increase in ROS production; the former ETosis is dependent on NADPH oxidase-mediated ROS, whereas the latter is the opposite. 3-MA as an autophagy inhibitor in the process of HET formation may hence be a suitable inhibitor for our study. This viewpoint, on the other hand, is further supported by the significant effect after treatment with rapamycin. It is unclear whether mTOR activity functions or autophagy regulation takes part in HET formation. We showed that, at least in the context of mTOR signaling, mTOR activity inhibition restricts the extracellular DNA via suppressing autophagy. In inflammatory sites, heterophils are likely to be exposed to multiple signals, which would activate various cellular functions cooperatively. Therefore, it will be a matter of further research.

NETosis has long been seen as a double-edged weapon, and autophagy-driven NETosis is no exception. The AMPK affects the GLUT4/GLUT1 expression and vesicles translocation to the plasma (Frøsig et al., 2010), both of which appear to increase glucose permeability. We found that glucose metabolism/transport contributes to FB_1-induced HET formation, as evidenced by the decreased effect of STF-31 and ritonavir. Notably, although STF-31 is a GLUT1 inhibitor, a recent finding has shown its dual role in Nicotinamide phosphoribosyltransferase (**NAMPT**) blocking cannot be underestimated (Adams et al., 2014). NAMPT is the bottleneck enzyme of the NAD salvage route, and intracellular NAD^+ is a cofactor required for glycolysis, pentose-phosphate pathway, and so on (Garten et al., 2015), indicating that NAMPT inhibition attenuates glycolysis/ROS in conjunction with HET blockade eventually (Ding et al., 2021). There is an alternative view that some NAMPT inhibitors could suppress ROS production while still killing bacteria (Roberts et al., 2013).

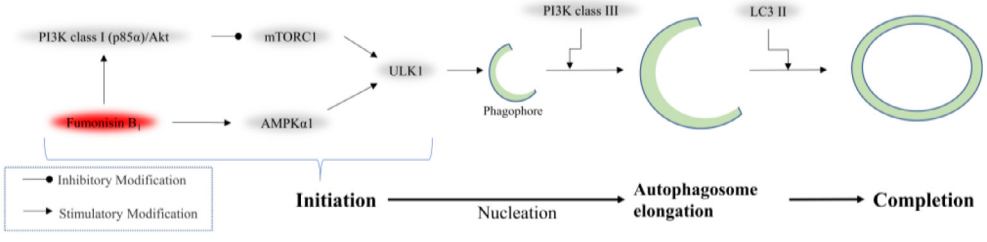

Figure 10. Schematic diagram illustrating the proposed mechanism of FB_1-induced heterophil autophagy.

Therefore, future research into NAMPT inhibitors' role in HET formation should be conducted. Second, we still felt obligated to investigate its precise procedure, such as the Rac1-GTPase in heterophils that control the glucose uptake indirectly, for the descriptions who also claim to have studied the correlation between them was extraordinarily close (Sylow et al., 2015). Rac1, a GTPase family member, is also one of the NADPH oxidase complex's regulatory components. Our result showed that the NSC23766-restrained Rac-GTPase resulted in a reduction in HET release. Rac proteins are expressed in neutrophils as three highly homologous proteins (Rac1, Rac2, and Rac3) (Dinauer, 2003). Our results aligned with Rac2 in NETs (Lim et al., 2011), indicating that Rac1 and Rac2 performed overlapping functions in NETosis.

After investigating the roles of HK2 and PFKFB3, we found that Bromopyruvic acid, 3PO decreased HET formation by FB_1 stimulation. This observation implied that glycolysis helped to maintain NETosis. The second group of the pharmacological assessment likewise revealed that AZD3965, which inhibits MCT1, abated the ETs formation, suggesting that circulating lactate, rather than glucose, would be a primary energy source for the tricarboxylic acid cycle in heterophil (Hui et al., 2017). Conclusively, understanding metabolic flexibility by lactate shuttles and metabolic checkpoints may open new avenues for developing therapies that target unregulated HET formation during various physiological conditions.

CONCLUSIONS

This study is expected to provide a theoretical basis for improving the role of FB_1 as an endocrine disruptor on the innate immune system. We described preliminary characters behind FB_1-triggered HET formation. The key mechanism of FB_1-triggered heterophil autophagy intertwined with HET formation. The lactate/glucose transporters and the nodal points of the glycolysis, like PFKFB3, affect HET release by controlling heterophil metabolism's initial and intermediate stages.

ACKNOWLEDGMENTS

This work was supported by the National Natural Science Foundation of China (No. 31772721).

DISCLOSURES

There are no conflicts of interest to declare.

SUPPLEMENTARY MATERIALS

Supplementary material associated with this article can be found, in the online version, at doi:10.1016/j.psj.2023.102511.

REFERENCES

Adams, D. J., D. Ito, M. G. Rees, B. Seashore-Ludlow, X. Puyang, A. H. Ramos, J. H. Cheah, P. A. Clemons, M. Warmuth, P. Zhu, A. F. Shamji, and S. L. Schreiber. 2014. NAMPT is the cellular target of STF-31-like small-molecule probes. ACS Chem. Biol. 9:2247–2254.

Arai, T., A. K. Bhunia, S. Chatterjee, and G. B. Bulkley. 1998. Lactosylceramide stimulates human neutrophils to upregulate Mac-1, adhere to endothelium, and generate reactive oxygen metabolites in vitro. Circ. Res. 82:540–547.

Axe, E. L., S. A. Walker, M. Manifava, P. Chandra, H. L. Roderick, A. Habermann, G. Griffiths, and N. T. Ktistakis. 2008. Autophagosome formation from membrane compartments enriched in phosphatidylinositol 3-phosphate and dynamically connected to the endoplasmic reticulum. J. Cell Biol. 182:685–701.

Barnes, K., J. C. Ingram, O. H. Porras, L. F. Barros, E. R. Hudson, L. G. Fryer, F. Foufelle, D. Carling, D. G. Hardie, and S. A. Baldwin. 2002. Activation of GLUT1 by metabolic and osmotic stress: potential involvement of AMP-activated protein kinase (AMPK). J. Cell Sci. 115:2433–2442.

Brinkmann, V., U. Reichard, C. Goosmann, B. Fauler, Y. Uhlemann, D. S. Weiss, Y. Weinrauch, and A. Zychlinsky. 2004. Neutrophil extracellular traps kill bacteria. Science 303:1532–1535.

Chen, J., J. Wen, Y. Tang, J. Shi, G. Mu, R. Yan, J. Cai, and M. Long. 2021. Research progress on fumonisin B1 contamination and toxicity: a review. Molecules 26:5238.

Dinauer, M. C. 2003. Regulation of neutrophil function by Rac GTPases. Curr. Opin. Hematol. 10:8–15.

Ding, J., Z. Zhang, W. Huang, and G. Bi. 2021. Nicotinamide phosphoribosyltransferase inhibitor is a novel therapeutic candidate in LPS-induced neutrophil extracellular traps. Microbiol. Immunol. 65:257–264.

Filomeni, G., D. De Zio, and F. Cecconi. 2015. Oxidative stress and autophagy: the clash between damage and metabolic needs. Cell Death Differ 22:377–388.

Frøsig, C., C. Pehmøller, J. B. Birk, E. A. Richter, and J. F. Wojtaszewski. 2010. Exercise-induced TBC1D1 Ser237 phosphorylation and 14-3-3 protein binding capacity in human skeletal muscle. J. Physiol. 588:4539–4548.

Garten, A., S. Schuster, M. Penke, T. Gorski, T. de Giorgis, and W. Kiess. 2015. Physiological and pathophysiological roles of NAMPT and NAD metabolism. Nat. Rev. Endocrinol. 11:535–546.

Geering, B., U. Gurzeler, E. Federzoni, T. Kaufmann, and H. U. Simon. 2011. A novel TNFR1-triggered apoptosis pathway mediated by class IA PI3Ks in neutrophils. Blood 117:5953–5962.

Germic, N., D. Stojkov, K. Oberson, S. Yousefi, and H.-U. Simon. 2017. Neither eosinophils nor neutrophils require ATG(5)-dependent autophagy for extracellular DNA trap formation. Immunology 152:517–525.

Hui, S., J. M. Ghergurovich, R. J. Morscher, C. Jang, X. Teng, W. Lu, L. A. Esparza, T. Reya, Z. Le, J. Yanxiang Guo, E. White, and J. D. Rabinowitz. 2017. Glucose feeds the TCA cycle via circulating lactate. Nature 551:115–118.

Itakura, A., and O. J. T. McCarty. 2013. Pivotal role for the mTOR pathway in the formation of neutrophil extracellular traps via regulation of autophagy. Am. J. Physiol. -Cell Physiol. 305:C348–C354.

Jewell, J. L., R. C. Russell, and K. L. Guan. 2013. Amino acid signalling upstream of mTOR. Nat. Rev. Mol. Cell Biol. 14:133–139.

Jiang, A., Y. Zhang, D. Wu, S. Li, Z. Liu, Z. Yang, and Z. Wei. 2021. Sodium molybdate induces heterophil extracellular traps formation in chicken. Ecotoxicol. Environ. Saf. 210:111886.

Kim, J., M. Kundu, B. Viollet, and K. L. Guan. 2011. AMPK and mTOR regulate autophagy through direct phosphorylation of Ulk1. Nat. Cell Biol. 13:132–141.

Knupp, J., F. Martinez-Montañés, F. Van Den Bergh, S. Cottier, R. Schneiter, D. Beard, and A. Chang. 2017. Sphingolipid accumulation causes mitochondrial dysregulation and cell death. Cell Death Differ 24:2044–2053.

Li, X. J., L. Deng, S. L. Brandt, C. B. Goodwin, P. Ma, Z. Yang, R. S. Mali, Z. Liu, R. Kapur, C. H. Serezani, and R. J. Chan. 2016. Role of p85α in neutrophil extra- and intracellular reactive oxygen species generation. Oncotarget 7:23096–23105.

Li, Y., and Y. Chen. 2019. AMPK and autophagy. Adv. Exp. Med. Biol. 1206:85–108.

Lim, M. B., J. W. Kuiper, A. Katchky, et al. 2011. Rac2 is required for the formation of neutrophil extracellular traps. J. Leukoc. Biol. 90:771–776.

Okkenhaug, K. 2013. Signaling by the phosphoinositide 3-kinase family in immune cells. Annu. Rev. Immunol. 31:675–704.

Ponce-Garcia, N., S. O. Serna-Saldivar, and S. Garcia-Lara. 2018. Fumonisins and their analogues in contaminated corn and its processed foods - a review. Food Addit. Contam. Part a-Chem. Analysis Control Expos. Risk Assess. 35:2183–2203.

Roberts, K. J., A. Cross, O. Vasieva, R. J. Moots, and S. W. Edwards. 2013. Inhibition of pre-B cell colony-enhancing factor (PBEF/NAMPT/visfatin) decreases the ability of human neutrophils to generate reactive oxidants but does not impair bacterial killing. J. Leukoc. Biol. 94:481–492.

Rodríguez-Espinosa, O., O. Rojas-Espinosa, M. M. Moreno-Altamirano, E. O. López-Villegas, and F. J. Sánchez-García. 2015. Metabolic requirements for neutrophil extracellular traps formation. Immunology 145:213–224.

Scott, P. M. 1993. Fumonisins. Int. J. Food Microbiol. 18:257–270.

Sylow, L., L. L. Møller, M. Kleinert, E. A. Richter, and T. E. Jensen. 2015. Stretch-stimulated glucose transport in skeletal muscle is regulated by Rac1. J. Physiol. 593:645–656.

Takei, H., A. Araki, H. Watanabe, A. Ichinose, and F. Sendo. 1996. Rapid killing of human neutrophils by the potent activator phorbol 12-myristate 13-acetate (PMA) accompanied by changes different from typical apoptosis or necrosis. J. Leukoc. Biol. 59:229–240.

Tan, V. P., and S. Miyamoto. 2015. HK2/hexokinase-II integrates glycolysis and autophagy to confer cellular protection. Autophagy 11:963–964.

Tanida, I., T. Yamaji, T. Ueno, S. Ishiura, E. Kominami, and K. Hanada. 2008. Consideration about negative controls for LC3 and expression vectors for four colored fluorescent protein-LC3 negative controls. Autophagy 4:131–134.

Thiel, P. G., W. F. Marasas, E. W. Sydenham, G. S. Shephard, and W. C. Gelderblom. 1992. The implications of naturally occurring levels of fumonisins in corn for human and animal health. Mycopathologia 117:3–9.

Wu, Z., X. Zhu, P. Li, X. Wang, Y. Sun, Y. Fu, J. Wang, Z. Yang, and E. Zhou. 2022. Fumonisin B(1) induces chicken heterophil extracellular traps mediated by PAD4 enzyme and P2 × 1 receptor. Poult. Sci. 101:101550.

Yan, S., X. Wei, S. Xu, H. Sun, W. Wang, L. Liu, X. Jiang, Y. Zhang, and Y. Che. 2017. 6-Phosphofructo-2-kinase/fructose-2,6-bisphosphatase isoform 3 spatially mediates autophagy through the AMPK signaling pathway. Oncotarget 8:80909–80922.

Yousefi, S., C. Mihalache, E. Kozlowski, I. Schmid, and H. U. Simon. 2009. Viable neutrophils release mitochondrial DNA to form neutrophil extracellular traps. Cell Death Differ. 16:1438–1444.

Zhou, E., I. Conejeros, Z. D. Velasquez, T. Munoz-Caro, U. Gaertner, C. Hermosilla, and A. Taubert. 2019. Simultaneous and positively correlated NET formation and autophagy in besnoitia besnoiti tachyzoite-exposed bovine polymorphonuclear neutrophils. Front. Immunol. 10:1131.